Technical Paper

Transactions of the Society of Naval Architects of Korea
Vol. 29, No.4, November 1992
大 韓 造 船 學 會 論 文 集
第 29 卷 第4號 1992 年 11 月

On the Added Resistance of SWATH Ships in Waves

by

Ho Hwan Chun*

파랑중에서 SWATH선의 부가저항에 관하여

전호환*

Abstract

This paper reports theoretical and experimental investigation into the added resistance of SWATH ships in waves. It was revealed from the experimental investigations on various SWATH models that the resistance of the SWATH models in waves is considerably reduced over part of the speed range as the wave height increases. As a first step to identify it, the first and second order wave forces have been investigated based on a linearised 3-D diffraction theory together with simplified boundary conditions and some results are reported herein. Also, the speed performance of SWATH ships in rough seas is compared with those of equivalent monohulls as well as with those of advanced high speed marine vehicles.

요 약

본 논문에서는 파랑중에서 소수선면 쌍동선(SWATH ship)의 저항증가에 관하여 해석적 및 실험적으로 다루었다. 여러가지 SWATH 모델들이 파고가 높아질수록 총저항이 정수중에서의 저항보다 적어진다는 특이한 현상들이 실험적으로 저자에 의해 보고되었다. 그 원인을 규명하기 위한 첫번째 단계로서 선형화된 3차원 diffraction 이론을 바탕으로 하여 SWATH선에 작용하는 1차 및 2차 힘들을 분석하였다. 또한 파랑중에서 SWATH선의 속도가 대응하는 단동선 및 다른 고속 선형에 비해 월등히 우세하다는 것을 보여준다.

발 표 : 1991년도 대한조선학회 추계연구발표회('92. 11. 16.)
Manuscript received : Dec. 2, 1991, revised manuscript received : August 1, 1992.
* Member, Hyundai Maritime Research Institute

1. Intooduction

The concept of the SWATH(Small Waterplane Area Twin/Triple Hull) ship has attracted considerable attention in the past two decades. Numerous advantages are claimed for the concept, including excellent motion characteristics at rest and underway, a high speed capability in waves, large deck area and greater design flexibility compared to its counterpart monohull. Today the interest in SWATH ships is rapidly growing and this is well reflected by the large number of publications on the subject in the technical press.

To promote SWATHs in the practical sense it is necessary to present seakeeping as part of an overall balanced design. This requires seakeeping performance to be a critical measure of the operational viability of a design in which the disadvantages of the SWATH concept have been accepted and minimized. Traditionally the design requirements do not pay adequate regard to speed loss in a seaway and this penalizes both the SWATH concept and the potential operator. Since SWATH ships are unlikely to be the preferred design for calm water situations it is not necessarily the case that calm water resistance is the appropriate criteria of performance. This paper demonstrates that the speed performance of SWATH ships in waves are much superior to those of equivalent monohulls as well as of other type of advanced marine vehicles.

SWATH ships are less likely to be forced to reduce speed because of unacceptable motions and additionally have a lower resistance augment in waves. The Japanese SSC Seagull is reported to have a speed loss of 2% in sea state 4[1] while the sea trial result of the Seagull Ⅱ revealed that her speed in seaways can be faster than that in calm water [2]. Experiments at Glasgov [3−6] with various SWATH models have shown that the resistance decreases dramatically(by up to as much as 24% of the calm water resistance) over some speed range in the super-critical zone, as the wave height increases. This result is very significant in the application of SWATHs to ship operations where speed loss is of prime importance. The research reported in this paper has been motivated by thses experimental findings in order to investigate the cause analytically. Indeed, it has been reported [7] that a component of radiated waves caused by a 2-D circular cylinder moving steadily with forced oscillation otherwise in calm water conveys negative wave energy and thus give negative added resistance at high Froude numbers. However, since the geometry of a SWATH is quite complicated and 3 dimensional, the problem is not as simple as with the 2-D cylinder.

The indirect boundary integral equation method (source distribution method) is applied to predict the 6 degree of coupled motions for SWATH ships travelling or stationary in waves from an arbitray heading. An existing linear 3-D diffraction theory together with the simplified boundary conditions is used to obtain the wave-exciting forces and hydrodynamic coefficients(added mass and damping). The viscous effect on the motions of SWATH ships is also taken into account by a semi-empirical method.

In general, there are two methods of solving the added resistance of vessels travelling in regular waves(or drifting force when the vessel is in stationary) ; the far and near field approaches. The far field approach derives the added resistance from consideration of conservation of either the total energy or the total momentum of the fluid. This method requires a knowledge of the total velocity potential and its derivatives far away from the vehicle. In contrast, the near field approach calculates the added force from the direct integration of the pressure on the wetted surface of the vessel. Both methods have advantages and disadvantages over the other. The near field approach requires more computational effort and is more unstable numerically compared to the far field. However, the vertical component of the drifting force can be examined with the near field approach. Using the near field approach, Pinkster[8] derived the drifting force for a floating body with

zero speed and Hearn et al[9] derived the added resistance for a ship with speed. The technical approach reported in this paper has been developed from those papers and reported in Ref.[10].

2. Mathematical Formulation

2.1 Coordinate system

Two sets of right handed reference systems are used. The first is the inertial axes system 0-xyz advancing in space with steady speed U, with x pointing towards the advancing direction, y to port and z upwards. The origin of this system is in the plane of the undisturbed free surface above the centre of gravity. The other axes system 0-$x'y'z'$ is fixed to the body. The two systems coincide with each other when there is no motion. For any point on the hull surface with position vector $\vec{r}$ in the body fixed system, its displacement from the 'at rest' position in the inertial frame can be expressed as:

$$\vec{\alpha} \cong \vec{\xi} + R_1\vec{r}' + R_2\vec{r}' + 0(\epsilon^3) \tag{1}$$

where $\vec{\xi}$ is the translational motion vector consisting of surge(ξ_1), sway(ξ_2) and heave(ξ_3), and R_1 and R_2 are the transformation matrices due to the translational and rotational movement of the body, respectively:

$$R_1 = \begin{bmatrix} 1 & -\xi_6 & \xi_5 \\ \xi_6 & 1 & -\xi_4 \\ -\xi_5 & \xi_4 & 1 \end{bmatrix} \tag{2}$$

$$R_2 = \begin{bmatrix} -\frac{1}{2}(\xi\frac{2}{5}+\xi\frac{2}{6}) & 0 & 0 \\ \xi_4\xi_5 & -\frac{1}{2}(\xi\frac{2}{4}+\xi\frac{2}{6}) & 0 \\ \xi_4\xi_6 & \xi_5\xi_6 & -\frac{1}{2}(\xi\frac{2}{4}+\xi\frac{2}{5}) \end{bmatrix} \tag{3}$$

where ξ_4, ξ_5 and ξ_6 are roll, pitch and yaw motions, respectively.

2.2 Exact Boundary Conditions

By assuming an inviscid, irrotational and incompressible fluid, the problem is reduced to solving a governing equation(Laplace's equation) which satisfies the following boundary conditions:

$$\begin{aligned} &\nabla^2\Phi = 0 && \text{in the fluid domain,} \\ &\triangle\Phi \cdot \vec{n} = 0 && \text{on the body surface,} \\ &\Phi_z = 0 && \text{at } z=-d \text{ on the seabed,} \end{aligned}$$

$$\left(\frac{\partial}{\partial t} - U\frac{\partial}{\partial x}\right)^2\Phi + 2\nabla\Phi\left(\frac{\partial}{\partial t} - U\frac{\partial}{\partial x}\right)\nabla\Phi + \frac{1}{2}\nabla\Phi\nabla(\nabla\Phi\nabla\Phi) + g\Phi_z = 0 \quad \text{at } z=\zeta(x,y) \tag{4}$$

and an appropriate radiation condition which makes the solution unique.

For the problem of a travelling vessel in waves, the velocity potential consists of three components:

$$\Phi(x,y,z,t) = -Ux + U\Psi(x,y,z) + \phi(x,y,z,t) \tag{5}$$

where the first term is due to the forward speed, the second term is called the steady perturbation potential due to the forward motion of the vessel and the last term is the unsteady velocity potential due to the incident and diffracted waves and induced motions in 6 degree of freedom.

2.3 Simplified Linearised 3-D Analysis

Since the boundary conditions above are highly nonlinear and furthermore, the free surface, $\zeta(x,y)$, is not known beforehand, it is nearly impossible to solve the problem directly. Therefore, an alternative method had to be found. A perturbation expansion scheme has been adopted introducing a small perturbation parameter. The physical meaning of the perturbation expansion is simple. When a vessel is advancing or is stationary in waves, some derivatives will develop around the vessel. These derivatives such as velocity potential, pressure, wave elevation, translational and angular motions, wetted surface area and normal direction etc, are of course functions of the vessel geometry

as well as of speed. It it is assumed, for example, that the vessel is very thin(ε=B/L is small), the derivatives will be consequently small up to moderately high speeds. The derivative can then be expanded into a series form given by:

$$D \cong \varepsilon^0 D^{(0)} + \varepsilon^1 D^{(1)} + \varepsilon^2 D^{(2)} + \cdots \tag{6}$$

where D indicates all derivatives around the vessel and 0, 1 and 2 indicate the zeroth, first and second order, respectively.

Now, the first order unsteady potential in eq. (5) can be expressed as:

$$\phi^{(1)} = [\phi^{(1)}_0 + \phi^{(1)}_7 + \sum_{j=1}^{6} \xi^{(1)}_j \phi^{(1)}_j] e^{-i\omega t} \tag{7}$$

where the first term is the first order incident wave potential as given by

$$\phi^{(1)}_0 = -\frac{ig\zeta_a}{\omega_0} e^{k_0 z} e^{ik_0(x \cos\beta + y \sin\beta)} \tag{8}$$

and the second term is the diffraction potential, and the last term is the potential due to jth mode of motion(j=1 denotes a surge motion, j=2 for sway, j=3 for heave, j=4 for roll, j=5 for pitch and j=6 for yaw). A body moving with constant speed U at an arbitrary angle β(180° for head waves) experiences waves of encounter frequency as

$$\omega = \omega_0 - U k_0 \cos\beta \tag{9}$$

where $k_0 = \omega_0^2/g$.

Neglecting the effect of the steady perturbation potential in eq.(5), which contributes to the wave-making resistance, and further, assuming that the forward motion is small and the frequency of oscillation is high, eq.(4) can be reduced to a well known simple form [11, 12, 13]:

$$-\omega^2 \phi^{(1)} + g\frac{\partial \phi^{(1)}}{\partial z} = 0 \text{ on } z=0 \tag{10}$$

Consequently, the speed dependent 1st order radiation potentials can be calculated as follows:

$$\phi^{(1)}_j = \phi^0_j \quad \text{for } j=1,2,3,4$$

$$\begin{Bmatrix} \phi^{(1)}_6 \\ \phi^{(1)}_5 \end{Bmatrix} = \begin{Bmatrix} \phi^0_6 \\ \phi^0_5 \end{Bmatrix} \pm \frac{U}{i\omega} \begin{Bmatrix} \phi^0_2 \\ \phi^0_3 \end{Bmatrix} \tag{11}$$

where ϕ^0_j are speed independent 1st order radiation velocity potentials.

3. 3-D Panel Source Distribution Method

By the virtue of Green's theorem, the velocity potential(both diffraction and radiation) can be expressed as follows:

$$\iint_S \sigma(Q) G(P,Q)\, ds(Q) = 4\pi \phi(P)$$

for P inside fluid (12)

where $\sigma(Q)$ is the source strength distributed over the mean wetted surface area of the body and G(P,Q) is the Green's function describing the influence at a point P(x,y,z) due to a unit source strength positioned at a point $Q(\xi,\eta,\zeta)$ on the body surface. The unknown source density can be found by imposing the boundary condition on the above equation and results in the following equation:

$$-\frac{1}{2}\sigma(P) + \frac{1}{4\pi}\iint_S \sigma(Q) \frac{\partial G(P,Q)}{\partial n}\, ds(Q) = v_n$$

for P on the body surface (13)

where v_n is the normal component of the velocity on the body surface.

Eq.(13) is the two dimensional Fredholm integral equation of the second kind which can be solved by various methods. Having found the source strength, the potential can be obtained by eq. (12) with the known source strength. The surface integral in eq.(13) can be written as the sum of the integrals over the N panels of area $\triangle S_j$ and, as an approximation, the source strength may be taken as constant over each panel. Then, eq.(13)

becomes,

$$-\frac{1}{2}\sigma_i+\frac{1}{4\pi}\sigma_j\iint_{\triangle S_j}\frac{\partial G}{\partial n}(x_i,y_i,z_i;\xi,\eta,\zeta)ds=v_{ni} \tag{14}$$

and similarly, eq.(14) can be written as:

$$\phi_i=\frac{1}{4\pi}\sigma_j\iint_{\triangle S_j}G(x_i,y_i,z_i;\xi,\eta,\zeta)ds \tag{15}$$

4. Pressure and Forces

The fluid pressure is given by the unsteady Bernoulli's equation,

$$P=-\rho[gz+\frac{1}{2}(\nabla\phi)^2+(\frac{\partial}{\partial t}-U\frac{\partial}{\partial x})\phi] \tag{16}$$

and the fluid force acting on the wetted surface is given by:

$$\vec{F}=\int_S P\,\vec{n}\,ds \tag{17}$$

where S is the instantaneous wetted surface and $\vec{n}$ is the instantaneous normal vector to the surface element ds relative to the inertial frame 0-xyz, directed inwards to the body surface.

Expanding the pressure and force as a perturbation expansion series as given in eq.(6), the forces of zero order to higher order, as desired, can be calculated by collecting terms of the same order. The detailed derivation can be seen in Ref. [10] and the final form of the mean second order force, which is of interest here, can be written in the following form:

$$\begin{aligned}\vec{F}^{(2)}=&\frac{1}{4}\rho g\oint_{L_0}|\zeta_r^{(1)}|^2\vec{n}_2^0\,dl\\&-\frac{1}{4}\rho\int_{S_0}|\nabla\tilde{\phi}^{(1)}|^2\vec{n}^{(0)}ds\\&+\frac{1}{2}Re\{\tilde{R}_1^*\vec{F}^{(1)}\}-\frac{1}{2}\rho\omega\\&\int_{S_0}Im\{\vec{\alpha}^{(1)*}\cdot\nabla\tilde{\phi}^{(1)}\}\vec{n}^{(0)}ds\\&+\frac{1}{2}\rho U\int_{S_0}Re\{\vec{\alpha}^{(1)*}\cdot\nabla\tilde{\phi}_x^{(1)}\}n^{(0)}ds\end{aligned}$$

$$+\frac{1}{2}\rho gA_w\,x_{c.f}\,Re[\tilde{\xi}_4^*\tilde{\xi}_6]\vec{k} \tag{18}$$

where the superscript~symbol denotes the complex amplitude of the variable, *the complex conjugate and

$$\vec{n}_2^{(0)}=(n_1^{(0)},n_2^{(0)},n_3^{(0)})/\sqrt{n_1^{(0)2}+n_2^{(0)2}}$$

$$\vec{\alpha}^{(1)}=\vec{\xi}^{(1)}+R_1\vec{r}$$

L_0 is the waterline contour of the ship in its equilibrium position in calm water, A_w is the waterplane area and $x_{c.f}$ is the longitudinal coordinate of the centre of floatation. ζ_r is the relative wave elevation due to the motion of the body and wave system and the first order relative wave elevation is given as

$$\zeta_r^{(1)}=\zeta^{(1)}-\xi_3-\xi_4y+\xi_5x \tag{19}$$

As seen in the above eq.(18), the total 2nd order force consists of 6 terms, each having its own physical meaning. The first component represents the contribution from the changing wetted surface area due to the relative free surface elevation. The second component is the effect of the square of the velocity in Bernoulli's equation indicating a pressure drop around the wetted surface of the hull. The third term is the effect of the first order fluid force due to the rotation of the body axis. The fourth component represents the change of the pressure gradient field on the wetted surface due to the body motion. The fifth term is called a convective term due to the steady forward speed. The last term accounts for the second order motion effect in rotation of the axis on the vertical force which becomes zero in head seas.

5. Computational Results and Discussion

In order to validate the present computational tool, the added resistance of a series 60 ship of C_B=0.7 has been calculated. The non-dimensional added resistance coefficient is shown as a function

of non-dimensional encounter frequency together with experimental results and other computational results [9] in Fig.1. In the figure and also throughout in this paper, the added resistance is taken to be positive when directed to leeward. Instead of using a length dimension(i.e., breadth or length of the ship) in non-dimensionalising the added resistance as usually used for monohulls, the displaced volume(∇) is employed for the present study :

$$C_{a.w}=R_{a.w}/0.5\ \rho g\zeta_a^2\nabla^{1/3}$$

The main reason for this is that the breadth of a SWATH ship is not directly characteristic of its displacement as it is for a monohull and that in this way, the added resistance of the two different type of ships(i.e., monohull and SWATH) can be compared quantitatively.

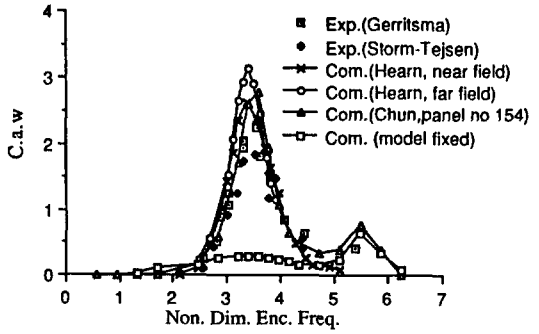

Fig.1 Added resistance coefficient of a series 60 ship of C_b=0.7 at Fn=0.207 in head seas

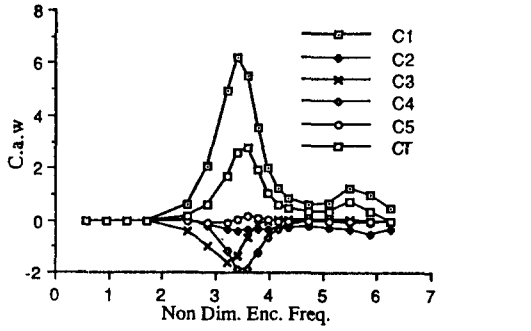

Fig.2 Added resistance coefficient components of a series 60 ship of C_b=0.7 at Fn=0.207 in head seas

From Fig.1, it can be seen that the present modelling gives good agreement with the experimental results as well as the other computational results. also, the figure shows how the first order motions influence the 2nd order force by looking at the added resistance for the fixed body(i.e., where only diffraction contributions has been calculated). Each component's contribution to the total added resistance, as given in eq.(18), is shown in Fig.2. As expected, it can be seen that most of the added resistance is contributed from the first term(C1) which is caused by the changed wetted surface area due to the relative free surface elevation. In general, an object floating in waves experiences a large difference in relative wave height between the seaward and leeward sides of the object so that this contribution is the largest. It is interesting to note that the total added resistance is less than the magnitude of the first term due to the negative contributions of the other terms. The sign of the each contribution term is dependent on the phase angles of the first order motions involved.

For various SWATH models[3-6], it has been found that there is little increase in the added resistance as speed increases. Furthermore, in the supercritical zone, as the wave height increases, the resistance decreases over part of the speed range. As a typical example, Fig.3 shows the total calm water resistance of SWATH-C5 against speed together with total resistances in waves of L_w/L_b= 1.0 for various wave heights. The SWATH model has a tandem strut configurattion with hulls of circular cross sections.

From Fig.3, it can be seen that as the wave height increases, the resistance decreases over the range of Fn=0.31-0.39 systematically with the tendency that the resistance peak shifts to the slower speeds and that the hollow and hump are flattened. This resistance decrease and trend has been found with the SWATH2 tandem strut rectangular hulled model over the same speed range [5] and also with the SWATH single strut fishing vessel over a similar speed range[4]. However, this

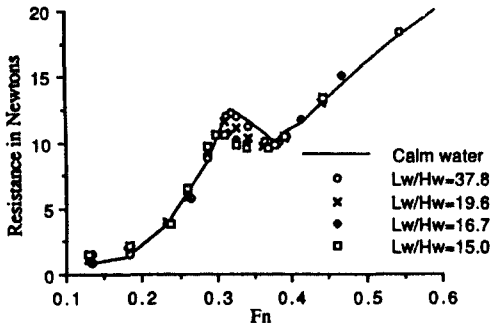

Fig.3 Total resistance of SWATH-C5 at L_w / L_b= 1.0

negative added resistance was not observed with the single strut SWATH3 model[3].

The non-dimensional added resistance coefficients of the SWATH1 model are plotted against speed in Fig.4 together with the computational results. It is generally believed that added resistance is proportional to the square of the wave height. If the square law is correct, then all the resistance of a given model at various wave heights but constant wave length can be reduced to a single curve when divided by the square of the wave heights. This is seen not to be the case.

From the figure, it is seen that the present diffraction theory does not give the negative added resistance results shown by the experiments. However, it is worthwhile mentioning that since motion responses of the model are very small at this wave encounter frequency, the energy loss due to the radiated waves is very low, even giving negative value(energy gain) at higher speeds. This phenomenon is exaggerated in Fig.5 which shows the added resistance coefficients of the SWATH1 model at the longer wave length of L_w/L_b=1.5. Over the speed range Fn=0.31−0.42 where negative added resistance also occurred, the radiated waves give negative energy to the model and thus, the total added resistance is reduced. This kind of phenomenon cannot be seen for the series 60 ship as shown in Fig.6 where the radiated waves contribute considerably to the total 2nd order force. As the encounter wave frequency increases, the diffraction force become dominant and at higher

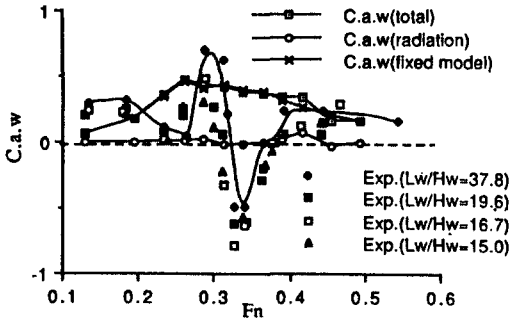

Fig.4 Added resistance coefficient of SWATH1-C5 vs Fn at wave freq. of L_w / L_b=1.0(head seas)

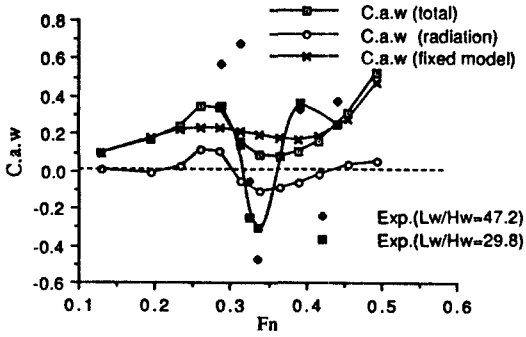

Fig.5 Added resistance coefficient of SWATH1-C5 vs Fn at wave freq. of L_w / L_b=1.5(head seas)

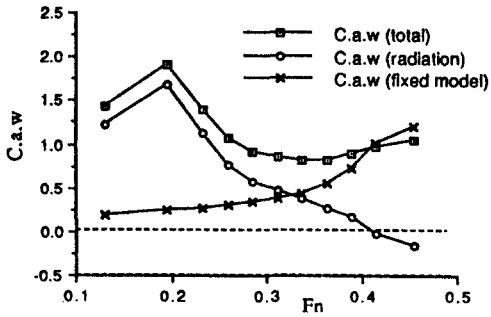

Fig.6 Added resistance coefficient of a series 60 ship of C_b=0.7 vs Fn at L_w / L_b=1.0 in head seas

encounter frequencies, the accuracy of computational results based on various linearised potential theories becomes worse as may be observed from Fig.1. Also, this accuracy is related to the panel number as well as panel size. For the present study, only one panel number for each model is used : panel number 154 for the series 60, 352 for the SWATH1 and 388 for the SWATH3 model.

The calm water resistance curves of all the models(SWATH1, SWATH2 and SWATH fishing vessel) which have negative added resistances, have a hump and hollow pattern over some speed range, typically as shown in Fig.3 for the SWATH1 model. However, the resistance of the SWATH3 increases monotonically with speed and the negative added resistance was not observed. The large peak of the SWATH1 model resistance around Fn= 0.32 in Fig.3 is caused by the interferences between various component of the model as can be clearly seen in Fig.7 which is taken from Ref. [14]. These interferences caused by the steady potential can be further interacted with the appearance of the unsteady potentials. Therefore, it can be postulated that the steady(wave-making resistance) component could be reduced to some extent when the model is towed in waves in a free mode. Also, the measured trim was reflected in a similar pattern showing that the trim in waves are reduced compared to that in calm water[14]. Even though the trim is caused by the vertical component of the hydrodynamic force while the resistance is the horizontal component, the different responses of the model could influence each other to some extent. Apart from this cause, some possible reasons for the negative zadded resistance can be stated as follows. There are some reports [15] that an airfoil(s) attached to the hull can create propulsive energy which moves the ship forward. By the same principle, the complicated hydrodynamic interferences between the many components of the tandem strut SWATH model combined with some motion aspects would create some propulsive forces. A steady suction force generated by the entrance of the submerged body in oscillation may also contribute partly.

Fig.8 show the calculated and measured added resistance coefficients of SWATH3-C1 vs non-dimensional encounter frequency at the speed of 1.0 m/sec(Fn=0.26). There is broad agreement between the computation and the experiments. The component contributions are drawn in Fig.9. The pattern of the added resistance for the SWATH3

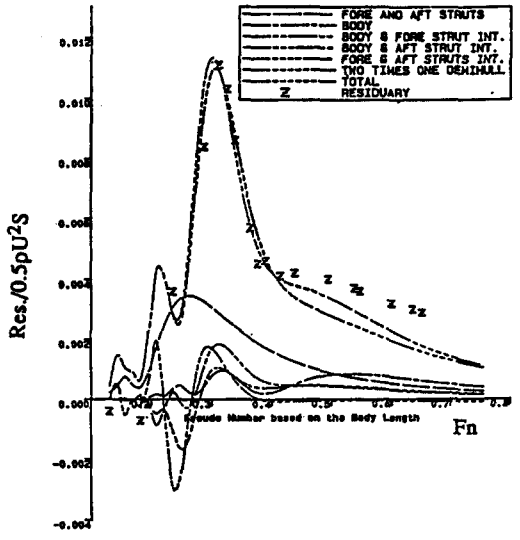

Fig.7 Wave resistance coefficients of SWATH1-C5 and its component variations together with residuary resistance coefficient vs Fn

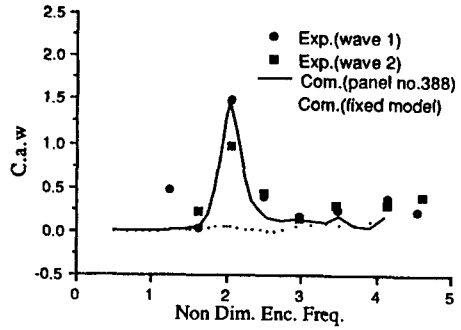

Fig.8 Added resistance coefficient of SWATH3-C1 and Fn=0.26

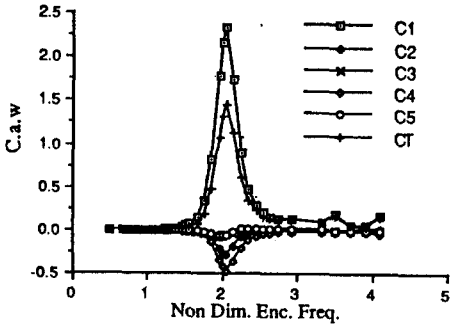

Fig.9 Added resistance coefficient components of SWATH3-C1 at Fn=0.26

is similar to that of the series 60 ship with some difference in the magnitude of the component contribution. C2, C3, C4 and C5 have all a beneficial influence on the added resistance for both the series 60 and SWATH3 ship, in particular, near heave resonance. For the series 60 ship, C4 and C3 are most beneficial and C2 becomes dominant at higher frequencies. However, for the SWATH3, C3 and C2 are most beneficial and C3 is small. This can be interpreted that the effect of the first order fluid force due to the rotation of the body axis is much smaller for the SWATH compared to the monohull and this seems to be due to a lower wave exciting force.

The surge, heave and pitch responses of the SWATH3-C1 at the same speed are shown in Figs. 10 to 12. The SWATH models tested were not fitted with fins and this explains the exceptionally low potential damping and the high resonant peaks (i.e., as much as three times the wave height in

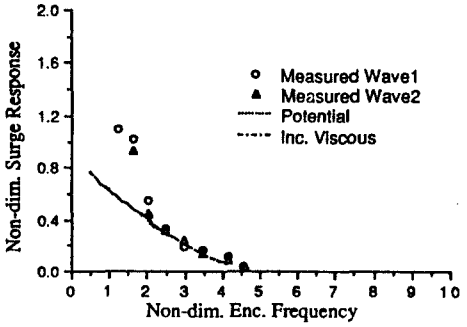

Fig.10 Surge response of SWATH3-C1 in head seas (Fn=0.26)

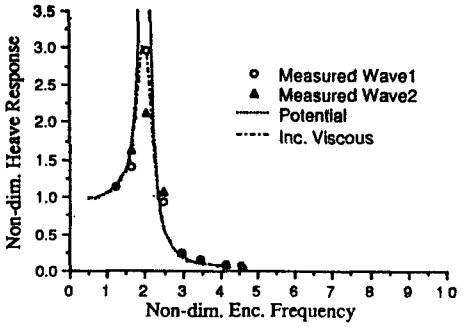

Fig.11 Heave response of SWATH3-C1 in head seas (Fn=0.26)

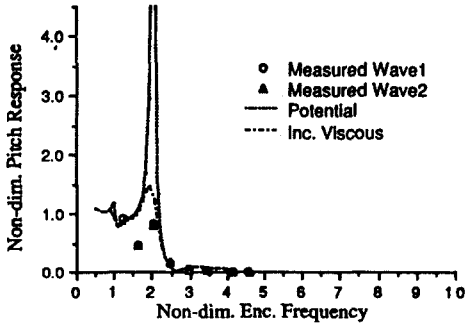

Fig.12 Pitch response of SWATH3-C1 in head seas (Fn=0.26)

heave response) in the model responses measured. Since the SWATH geometry is quite different from that of the monohull, as usual, the potential only damping is not enough to predict the motion responses well near the resonant frequency. Therefore, an empirical viscous damping factor was added. This was described fully in Ref.[16]. As seen in the figures, the predicted motion responses with the empirical viscous damping agree well with the experimental results near the resonant region. Since the second order forces are very sensitive to the first order responese(force, motion and phase, etc), correct values should be used. Therefore, the added resistance of the SWATH models reported in this paper is always calculated based on the first order forces with the empirical viscous damping.

6. Performance Comparison of SWATH Ships with Other Type of Marine Crafts

Fig.13 shows the comparison of measured total resistances(per unit displacement) in calm water and in waves of three model, the single strut SWATH3-C1, Destroyer DE-1006(C_b=0.49) and Series-60(C_b=0.7). The length(1.52m) of DE-1006 and Series-60 is nearly the same as that of the SWATH1 model(1.51m). This coincidence enables the present comparison to be much more reliable because the Reynolds number is nearly the same at the same speed for all models.

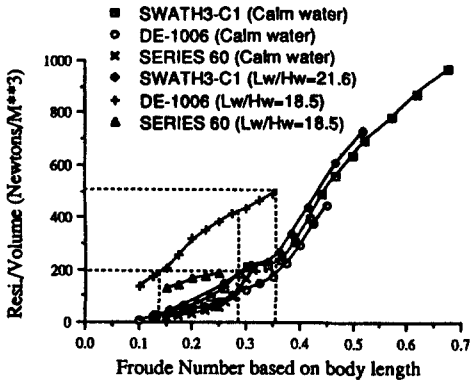

Fig.13 Comparison of resistances(per unit displacement) of three models : SWATH3-C1, Destroyer DE-1006 and Series 60(C_b=0.7)

As seen in the figure, the calm water resistance of the SWATH model is greater than those of the Destroyer and Series-60 at all the speeds tested. However, the resistance of the Series-60 would be greater than that of the SWATH above Fn=0.31(generally known as the wave 'barrier'). Beyond that speed, the resistance increase of such a type of vessel is so steep that in practice, they are not economical. Expect with the hump speed range which is caused by the interference effects between the body and strut as mentioned above, the resistance per unit displacement of the SWATH model is 8-10% greater than that of DE-1006 at high speeds and 10-20% at slow speeds.

However, in waves, the story is dramatically changed. At a similar wave steepness to that for the SWATH model, the resistance of DE-1006 is increased so much that, for instance, by the same power marked on the figure, the SWATH runs at speed of Fn=0.285 while DE-1006 runs at speed of Fn=0.14. In other words, when the Destroyer DE-1006 changes from calm water to waves with a steepness of around L_w/H_w=18.5, her speed will be involuntarily reduced from Fn=0.36 to Fn=0.14(more than 61% reduction). Or, in order to maintain the calm water speed, the power should be increased up to more than 500 newtons per unit displacement(i.e., more than 270% increase). However, at this speed, there is little resistance increase for the SWATH3 due to the waves. Therefore, in order to keep the speed of Fn=0.285 at sea whose conditions is similar to that given here, the power of the SWATH is around 60% less than that of the Destroyer.

This fact can be well illustrated by the service experience of the SWATH PATRIA, F.B.M. Marine Ltd., U.K[17]. The vessel entered service on August 19, 1990 operating between Funchal and Porto Santo off the Island of Maderia in the Atlantic, which is also served by a conventional catamaran, the Westamaran 100. Table 1 shows the operating time comparison of the two crafts in various sea conditions, summarised from Ref. [17]. The SWATH ship completed the crossing in an average time of 1 hour 35 minutes in conditions up to 2.0m seas and 1 hour 39 minutes in 2.0−3.0m seas. The corresponding times for the Westamaran 100 catamaran are 1 hour 45 minutes in up to 1.0m seas, 2 hours in 1−2m seas and 2 hours 20 minutes in 2−3m seas. It is also reported that seasickness levels has fallen in 2−3 m seas from around 50−60% on the Westamaran 100 to 10−15% on the SWATH PATRIA.

G.Nigel introduced a handy method of assessing the merits of various competing designs, as shown in Table 2 taken from Ref.[18]. From the table, it can be seen that no other type of crafts can compete with the SWATH ship in terms of speed performance and comfortness.

Table 1 Compsrison of running time and sea sickness of the SWATH PATRIA and the Westamaran 100 catamaran

	Running Time	
Sea conditions	SWATH PATRIA	Westamaran 100
−1.0m seas		1 hrs 45 minutes
−2.0m seas	1 hr 35 minutes	2 hrs
−3.0m seas	1 hr 39 minutes	2 hrs 20 minutes
Sea sickness (2−3m seas)	10−15%	50−60%

Table 2 Taken from Ref.[18]

Parameter	SES	Cat	Mono	Hydro	SWATH
calm water speed	1	2	4	3	4
speed in sea state 5:					
head seas	5	4	3	2	1
beam seas	3	2	4	4	1
following seas	3	2	3	4	1
speed degradation:					
head seas	5	4	3	2	1
beam seas	4	3	4	1	2
following seas	4	2	3	4	1
comofort:					
head seas	5	4	3	2	1
beam seas	4	2	5	4	1
following seas	3	2	3	4	1
internal noise	5	1	2	3	3
maintenance:					
ease and cost	5	2	1	4	2
operational ease and cost	5	2	1	4	2
transport efficiency	5	1	2	3	2
commercial effi.	5	2	1	4	3
total	62	35	42	48	26
total with speed weighting	71	53	73	75	62

$$\text{Commercial efficiency} = \frac{\text{revenue payload} \times \text{average sea state cruising speed}}{\text{capital cost}}$$

$$\text{Transport efficiency} = \frac{\text{revenue payload} \times \text{average sea state cruising speed}}{\text{installed horsepower}}$$

7. Conclusions

From the experimental and computational results as well as data of service experience, the present paper demonstrated that SWATH ships can sustain their speed with only little loss in waves. The power requirement of the SWATH ship in calm water is more or less greater than those of other type of equivalent marine crafts. However, its power requirement in waves is very much smaller than that of the equivalent counterpart. Although the added resistance is only a part of the total resistance, ships in general operate in wave conditions. With regard to this, the slightly higher calm water resistance of the SWATH ship may be trivial compared to the power increase of the equivalent counterpart in waves. In conclusion, it can be said that the design power requirement for a SWATH ship may be much less than those of equivalent other type of surface running crafts at seas.

With regard to the negative added resistance, unlike the monohull, the second order force due to the radiated waves of the SWATH model is negligible and even gives negative values(energy gain) over the speed range Fn=0.3−0.42 where a large resistance reduction occurred. However, due to the large contribution from the diffraction waves, the present theory does not give negative added resistance. As discussed in detail in the section 5, the calm water resistance curves of all the models, SWATH1, SWATH2 and SWATH fishing vessel, with which negative added resistance occurred, have a hump and hollow pattern which is caused by the interference between the several component of the models. These interferences caused by the steady potential can be further affected by the appearance of the unsteady potentials due to waves. Thus, the steday wave-making resistance can be changed when the model is towed in waves in a free mode. Therefore, in order to investigate fully the negative added resistance problem, it can be recommended that the interference between the steady and unsteady potentials be fully taken into account.

References

[1] Narita H. et al, 'Design and full scale test results for SSC vessels', 1st Int. MSDC Conf., London, April, 1982.

[2] Yaki H. and Masuyama K., 'Experiences of Motion Characteristics of High-Speed SWATH', Proc. of Korea-Japan Joint Workship on Hydrodynamics in Ship Design, Seoul National University, Seoul, Korea, June 1991.

[3] Chun H.H. et al, Proc. of 22nd ATTC, pp. 464−472, St John's, Canada, Aug. 1989.

[4] Djatmiko E.B., Chun H.H. et al, 'Hydrodynamic Behaviour of a SWATH Fishing Vessel', Proc. of CSME Mechanical Engineering Forum, Toronto, June, 1990.

[5] Chun H.H. et al, 'On Reduced Resistance of SWATH Model in Waves', Journal of AIAA, Vol.29, No.5, May 1991.

[6] Chun H.H. et al, 'Experiments on the Added Resistance of SWATH Models in Regular Head Waves', Proceedings of 19th ITTC, HSMV Committee, Madrid, Spain, Sep., 1990.

[7] Grue J. and Palm E.J. Fluid Mech., Vol.151, pp.257-278, 1985.

[8] Pinkster J.A., Low Frequency Second Order Wave Exciting Forces on Floating Structures, NSMB report 650, 1980.

[9] Hearn G.E., Tong K.C. et al, Proc. of the ASME Int. Conf. on Offshore Mechanics and Arctic Engineering, pp.213--225, Houston, U.S.A., March 1987.

[10] Chun H.H. and McGregor R.C., 'First and Second Order Force on SWATH Ships in Waves', IUTAM Symposium on Dynamics of Marine Vehicles and Structures in Waves, Brunel Univeristy, London, June 1990.

[11] Salvesen N., Tuck E.O. and Faltinsen O., Trans. SNAME, pp.250-279, Vol.78, 1970.

[12] Inglis R.B., Three-Dimensional Analysis of the Motion of a Rigid Ship in Waves, Ph.D Thesis, Univ. College London, U.K., 1980.

[13] Chun H.H. et al., 'A Wide Ranging Study on the Motions of SWATH Ships with and without Forward Speeds', Proceedings of the ASNE 9th Int. Conference on OMAE, Houston, Feb., 1990.

[14] Chun H.H., 'Theoretical and Experimental Studies on the Resistance of SWATH Ship's, Ph.D. Thesis, University of Glasgow, U.K., 1988.

[15] Isshiki H. and Murakami M., 'Wave Power Utilisation into Ship Propulsion', 5th Int. Sym.and Exihibition on Offshore Mechanics and Arctic Engineering (OAME), Toyko, 1986.

[16] Chun H.H., '2nd Order Forces and Moments for Floating Structures', Report to YARD Ltd, U.K., Nov. 1989.

[17] Milner R., 'Service Experience of the Seamaster Fast Displacement Catamaran(SWATH) Ferry', Cruise+Ferry 91, London, May 1991.

[18] Nigel G., 'Design for Speed, Economy and Comfort-The Role of the Independent Designer in the Design of High Speed Surface Craft', Pro. of the 7th Int. High Speed Surface Craft Conference, London, 1990.